



## Catalytic ozonation of antipyrine with a magnetic core/shell CeO<sub>2</sub> catalyst: kinetics and mechanism

Liling Chen, Siqi Fan, Pan Xiong, Jinshan Song, Qizhou Dai\*

College of Environment, Zhejiang University of Technology, Hangzhou 310032, China, Tel. +86 571 88320276;  
Fax: +86 571 88320882; email: dqz@zjut.edu.cn (Q. Dai)

Received 30 April 2020; Accepted 17 October 2020

### ABSTRACT

In this study, antipyrine was selected as the typical pharmaceutical and personal care products (PPCPs) and the abatement of antipyrine was investigated by the catalytic ozonation with a magnetic Fe<sub>3</sub>O<sub>4</sub>@SiO<sub>2</sub>@CeO<sub>2</sub> catalyst. Focusing on the kinetics of the antipyrine degradation at different initial concentrations of antipyrine, the ozone dosages, initial pH values, the antipyrine degradation mechanism, and catalytic mechanism was explored. The results showed that the core/shell Fe<sub>3</sub>O<sub>4</sub>@SiO<sub>2</sub>@CeO<sub>2</sub> catalyst exhibited high activity in the degradation of antipyrine. Types of intermediates, such as anisole, nitrobenzene, *n*-phenylpropinamide, and aniline were detected by gas chromatography–mass spectrometry and high performance liquid chromatography techniques during the catalytic ozonation process. The presence of the radical scavenger *tert*-butyl alcohol during catalytic ozonation promoted the degradation of antipyrine unexpectedly instead of inhibiting the generation of hydroxyl radicals from ozone decomposition. The results implied that the high removal efficiency was mainly attributed to the interfacial effect of Fe<sub>3</sub>O<sub>4</sub>@SiO<sub>2</sub>@CeO<sub>2</sub> catalyst. The energy consumption was also analyzed and discussed. This paper could provide basic data and technique reference of catalytic ozonation for the PPCPs wastewater treatment.

**Keywords:** Catalytic ozonation; Antipyrine; Intermediates; Mechanism; Energy consumption

### 1. Introduction

The pollution control of pharmaceutical and personal care products (PPCPs) has been one of the hottest research topics over the past decades [1–4]. Although low concentrations of PPCPs in the aquatic environment have been detected, potential risk on human health still needs to be considered because of widely varying types and certain chemically and biochemically-persistent properties [5,6]. The inappropriate usage or disposal of PPCPs has become an emerging worldwide problem. Antipyrine, a typical PPCP, is widely used as an antipyretic and analgesic drug (poly pill) to treat cold and headache [7]. Now, the antipyrine production is growing annually because contemporary people weaker and more likely to get ill than before due to irregular and unhealthy lifestyle. China has become

the largest producer of antipyretic analgesics in the world. However, the study of pollution control of antipyrine is still limited in China.

Advanced oxidation processes, such as Fenton, and electrochemical oxidation, have been proposed to deal with aqueous solution containing PPCPs [8,9], but the available methods to treat antipyrine (AP) are still limited. At present, UV and ozonation for the AP degradation have been mentioned [10,11], so it is still a long way away from our expectation to transform it into less toxic and more biodegradable intermediates. Here's how our idea compares to other people's approaches. Advanced oxidation processes for the treatment of refractory compounds are effective and have been commonly utilized [12,13], especially catalytic ozonation due to high destructive ability [14]. Although the separation of the catalysts and the utilization of ozone

\* Corresponding author.

are the remaining issues, a lot of researches still pay much attention for catalytic ozonation [15]. In heterogeneous catalytic ozonation, supported and unsupported metal oxides are one kind of the most common catalysts to treat with these compounds [16,17], especially the magnetic particle catalysts which have been prepared and studied in recent years because of their magnetic, electric, and dielectric properties [18]. It has been reported about the application of  $\text{Fe}_3\text{O}_4$ ,  $\text{Fe}_2\text{O}_3$ , and some supported iron oxides in the catalytic ozonation process, but it was found little effect on the removal rate of organic matters. The core/shell composite microspheres which were integrated by the combination of mesoporous silica and magnetic particles were of great interest for their unique magnetic responsivity and chemically modifiable surface [19]. Besides,  $\text{CeO}_2$  was often employed on kinds of catalysts, exhibiting favorable activity because of its ability to absorb and release oxygen, and has been applied in catalysis, sensing, and fuel cells [20]. Therefore, we decided to combine the structure of core/shell microspheres with other materials and finally made it with a synthesis of the  $\text{Fe}_3\text{O}_4@\text{SiO}_2@\text{CeO}_2$  catalyst. The detailed preparation system has been established previously and the performance of  $\text{Fe}_3\text{O}_4@\text{SiO}_2@\text{CeO}_2$  catalyst for the removal of acetylsalicylic acid was tested with promising results [21].

In the study, we selected the antipyrine as the model PPCP and explore catalytic ozonation with  $\text{Fe}_3\text{O}_4@\text{SiO}_2@\text{CeO}_2$  catalyst for the treatment of the pharmaceutical substance wastewater. The effects of the operational factors were optimized and the antipyrine degradation mechanism was explored with the analysis of a kind of intermediates. The catalytic ozonation mechanism with  $\text{Fe}_3\text{O}_4@\text{SiO}_2@\text{CeO}_2$  catalyst was also investigated and the energy consumption was discussed. This paper could give basic data and technique references for PPCP wastewater pollution control.

## 2. Experimental

### 2.1. Chemicals and catalysts

The model pollutant antipyrine (AP) was obtained from Aladdin Reagent (China) Co., Ltd., *tert*-butyl alcohol (TBA) was purchased from Shanghai Lingfeng Chemical Reagent (China) Co., Ltd. All other chemicals which were of analytical grade were supplied by Huadong Medicine (China) Co., Ltd., and used without further purification. Ultrapure water was utilized for the preparation of solutions. The initial pH of solutions was adjusted by a pH meter (PB-21, Sartorius, China).

The  $\text{Fe}_3\text{O}_4@\text{SiO}_2@\text{CeO}_2$  nanoparticles applied in the experiments were synthesized by hydrolysis precipitation method, which involved the preparation of magnetic  $\text{Fe}_3\text{O}_4$  nanoparticles by the titration hydrolyzation method, coating with a  $\text{SiO}_2$  layer through a sol-gel approach, a mesoporous  $\text{CeO}_2$  shell subsequently loaded on the outermost layer by chemical precipitation and final calcination in the tube furnace. The detailed preparation of the  $\text{Fe}_3\text{O}_4@\text{SiO}_2@\text{CeO}_2$  nanoparticles, the morphology, structural analysis, and the stability of the catalyst were elaborated in our previous work [21]. The characteristic of the  $\text{Fe}_3\text{O}_4@\text{SiO}_2@\text{CeO}_2$  nanoparticles was tested and the  $S_{\text{BET}}$  value was  $195 \text{ m}^2 \text{ g}^{-1}$ , the average pore size was 2.6 nm and

point of zero charge was 3.46 [22]. The saturation magnetization values of  $\text{Fe}_3\text{O}_4$ ,  $\text{Fe}_3\text{O}_4@\text{SiO}_2$ , and  $\text{Fe}_3\text{O}_4@\text{SiO}_2@\text{CeO}_2$  were 62.8, 46.0, and  $47.7 \text{ emu g}^{-1}$ , respectively [23].

### 2.2. Experiments

Catalytic ozonation experiments were conducted at room temperature to observe the performance of the magnetic nanoparticles for AP removal in a cylindrical Pyrex glass reactor. The reaction volume is 1.5 L. Different concentration aqueous solution of AP (initial concentrations from 100 to  $1,000 \text{ mg L}^{-1}$ , mostly is  $1,000 \text{ mg L}^{-1}$ ) was introduced into the reactor and bubbled with oxygen continuously in favor of well-diffusion of catalysts. The catalysts (mostly at an approximate dose of  $666 \text{ mg L}^{-1}$  unless specified) were added instantly into the reaction solution with the starting of the ozone generator (CFY-3, Hangzhou Rongxin Electronic Equipment Co., Ltd., China) simultaneously. The ozone dosage was controlled by adjusting the rotameter. Samples were withdrawn at each time-point and then filtered through  $0.22 \mu\text{m}$  pore size membrane filters after the quenching of the residual ozone by adding  $0.1 \text{ M Na}_2\text{S}_2\text{O}_3$ . Mechanism study was conducted at an initial pH in the presence of  $\text{Fe}_3\text{O}_4@\text{SiO}_2@\text{CeO}_2$  catalyst for 2 h.

### 2.3. Analytical methods

The concentration of antipyrine was measured by high performance liquid chromatography (HPLC) (Model 1200, Agilent Technologies, USA) that consisted of a C18 reversed-phase column ( $250 \text{ mm} \times 4.6 \text{ mm} \times 5 \mu\text{m}$ , Agilent Technologies) and a UV detector. The mobile phase was composed of methanol and water at 40:60 (v/v) (room temperature). The flow rate was set at  $1 \text{ mL min}^{-1}$  and the absorption wavelength was measured at 241 nm. Chemical oxygen demand (COD) was determined via the spectrophotometric method at 610 nm using a HACH chromometer (HACH DRB200, USA) based on rapid-digestion method. The intermediates produced in catalytic ozonation process were analyzed by a gas chromatography-mass spectrometry (GC-MS) with DB-5MS capillary column ( $30 \text{ m} \times 0.32 \text{ mm} \times 0.25 \mu\text{m}$ ). The procedure was programmed at initial temperature  $50^\circ\text{C}$  for 1 min, then increased to  $250^\circ\text{C}$  at the rate of  $10^\circ\text{C min}^{-1}$  and kept for 5 min. The split rate was 5:1.

## 3. Results and discussion

### 3.1. Effectiveness

In this study, the effect of  $\text{Fe}_3\text{O}_4@\text{SiO}_2@\text{CeO}_2$  nanoparticle catalyst was evaluated for the catalytic ozonation of antipyrine (AP) and COD removal shown in Fig. 1. The results showed that the AP removal rate in the catalytic ozonation with magnetic catalysts was superior to ozonation alone. Among these, the maximum removal rate of 88% could be achieved by  $\text{Fe}_3\text{O}_4@\text{SiO}_2@\text{CeO}_2$ . However, when  $\text{Fe}_3\text{O}_4@\text{SiO}_2@\text{CeO}_2$  was used alone, only around 4% of AP was removed (not shown), suggesting its negligible AP adsorption capacity. The COD removal was observed under the same conditions and followed the same trend. The addition of magnetic catalysts enhanced the COD

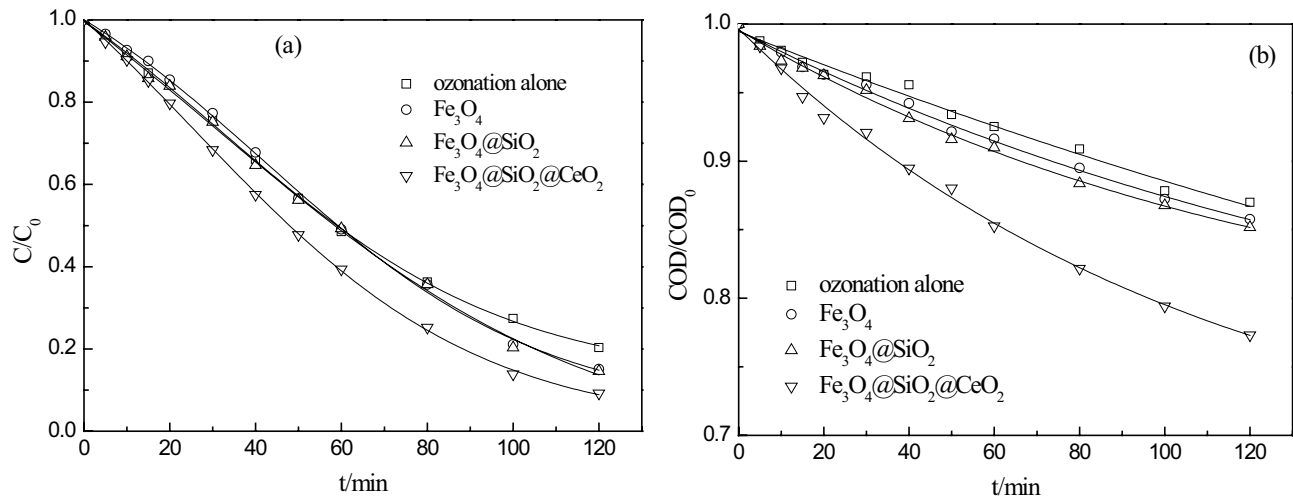


Fig. 1. Influence of  $\text{Fe}_3\text{O}_4$ ,  $\text{Fe}_3\text{O}_4@\text{SiO}_2$ , and  $\text{Fe}_3\text{O}_4@\text{SiO}_2@\text{CeO}_2$  nanoparticles catalysts in ozonation process: (a) AP removal and (b) COD removal. Experimental conditions:  $C_0 = 1,000 \text{ mg L}^{-1}$ ,  $Q_{\text{O}_3} = 8 \text{ mg min}^{-1}$ , and catalytic dosage  $\approx 666 \text{ mg L}^{-1}$ .

removal rate, 14.2% with  $\text{Fe}_3\text{O}_4$ , 14.8% with  $\text{Fe}_3\text{O}_4@\text{SiO}_2$ , and 22.7% with  $\text{Fe}_3\text{O}_4@\text{SiO}_2@\text{CeO}_2$ , only 13.1% by ozonation alone after 120 min. This indicated that  $\text{Fe}_3\text{O}_4@\text{SiO}_2@\text{CeO}_2$  nanoparticle catalyst seemed to be a good catalyst for the AP degradation. In comparison, the COD removal rate was much less than the AP removal rate, which explained that amounts of intermediates were produced in the conversion process of AP.

### 3.2. Optimization of operational factors

To investigate the influence of various parameters on the degradation of antipyrine (AP) and the removal of COD, batch catalytic ozonation tests were carried out under different conditions with  $\text{Fe}_3\text{O}_4@\text{SiO}_2@\text{CeO}_2$ . The degradation kinetics of antipyrine (AP) was also investigated. It was found that kinetics discoloration of antipyrine (AP) during catalytic ozonation corresponded to the pseudo-first-order model. We can have a clear understanding of the influence of variables and the optimization of operational parameters from kinetic constants of ozone oxidation reaction. Therefore, the pseudo-first-order kinetic Eqs. (1)–(3) were used to fit the experimental data [24]:

$$\frac{d[C]}{dt} = -k_{\text{O}_3}[C][\text{O}_3] - k_{\text{OH}}[C][\cdot\text{OH}] \quad (1)$$

$$\frac{d[C]}{dt} = -(k_{\text{O}_3}[\text{O}_3] + k_{\text{OH}}[\cdot\text{OH}])[C] \quad (2)$$

$$\ln \frac{C_0}{C} = kt \quad (3)$$

where  $[\text{O}_3]$ ,  $[\cdot\text{OH}]$ , and  $[C]$  are the concentrations of ozone,  $\cdot\text{OH}$  and AP in the solution, respectively. The  $k_{\text{O}_3}$  and  $k_{\text{OH}}$  are the kinetic reaction constants of AP with  $\text{O}_3$  and  $\cdot\text{OH}$ .  $C_0$  and  $C$  are the concentrations of AP at reaction time (0) and ( $t$ ),  $k$  is pseudo-first-order rate constant ( $\text{min}^{-1}$ ),  $t$  is the reaction time.

#### 3.2.1. Influence of initial AP concentration

Fig. 2 shows the influence of different initial AP concentrations on AP degradation in  $\text{O}_3/\text{Fe}_3\text{O}_4@\text{SiO}_2@\text{CeO}_2$  system. The results showed that the increase of initial AP concentrations from 100 to 1,000  $\text{mg L}^{-1}$  reduced the AP removal rate, after 30 min of reaction, 99.24% removal of AP decreased to 26.48%. On condition of 100  $\text{mg L}^{-1}$ , the AP removal rate could reach 100% after 40 min. Kinetics investigation of AP degradation with the initial concentration in this range was performed and the results indicated that the AP degradation followed the pseudo-first-order model with good correlation coefficients over 0.99. The relevant apparent rate constant decreased from  $6.85 \times 10^{-2}$  to  $1.19 \times 10^{-2} \text{ min}^{-1}$  with the initial AP concentration.

#### 3.2.2. Influence of the ozone dosage

Over half of AP removal always occurred within 60 min of reaction in  $\text{O}_3/\text{Fe}_3\text{O}_4@\text{SiO}_2@\text{CeO}_2$  system as shown in Fig. 3. The positive effect of the ozone dosage on the AP degradation was observed from the beginning of the experiment. When the ozone dosage increased from 8 to 40  $\text{mg min}^{-1}$ , the AP removal rate after 30 min was 26.48%, 56.84%, 75.4%, 85.23%, and 99.05%, respectively, as aqueous ozone concentration increased with the increase of the ozone dosage. As shown in Fig. 3, the AP removal got a good fitting and the pseudo-first-order rate constants of catalytic ozonation of AP increased obviously with the variation of the ozone dosage which ranged from  $1.19 \times 10^{-2}$  to  $9.76 \times 10^{-2} \text{ min}^{-1}$ .

#### 3.2.3. Influence of the catalyst dosage

To effectively verify the catalytic activity, the catalyst dosage from 0 to 1.0 g on the AP degradation was discussed. Fig. 4 shows the variation of AP and COD removal rate in  $\text{O}_3/\text{Fe}_3\text{O}_4@\text{SiO}_2@\text{CeO}_2$  system. The result showed that the increase of the catalyst dosage obviously improved the AP removal and the AP removal rate in catalytic ozonation was 9% higher than that in ozonation alone (Fig. 4a).

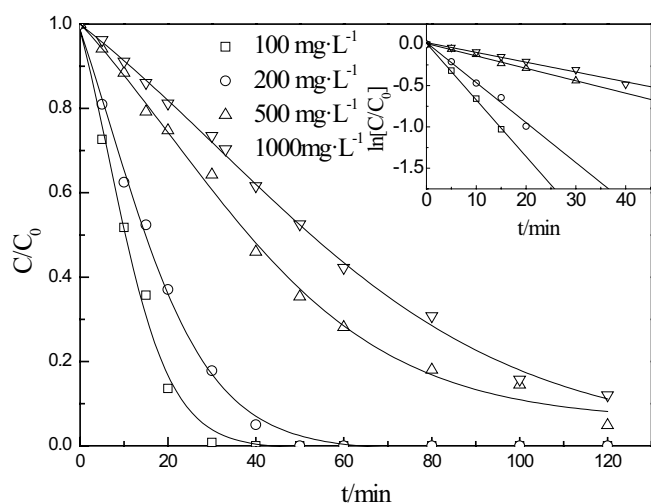


Fig. 2. Influence of initial concentration of AP in catalytic ozonation process on AP removal. Experimental conditions:  $Q_{O_3} = 8 \text{ mg min}^{-1}$ ,  $\text{pH} = 7.2$ , and catalytic dosage  $\approx 666 \text{ mg L}^{-1}$ .

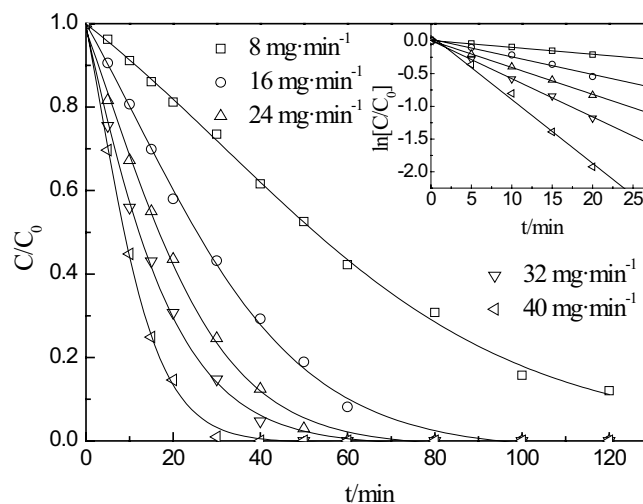


Fig. 3. Influence of the ozone dosage in catalytic ozonation process on AP removal. Experimental conditions:  $C_0 = 1,000 \text{ mg L}^{-1}$ ,  $\text{pH} = 7.2$ , and catalytic dosage  $\approx 666 \text{ mg L}^{-1}$ .

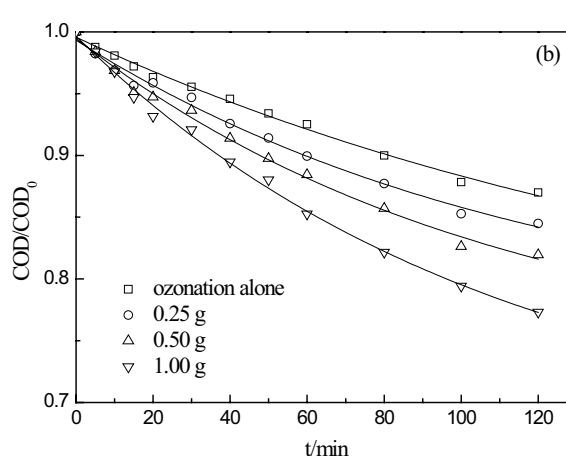
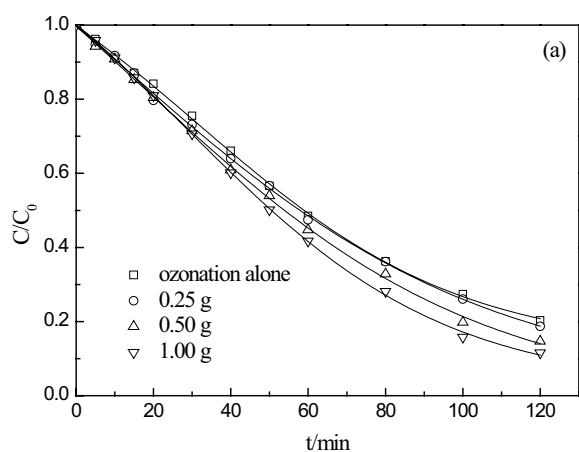


Fig. 4. Influence of the catalyst dosage in catalytic ozonation process: (a) AP removal and (b) COD removal. Experimental conditions:  $C_0 = 1,000 \text{ mg L}^{-1}$ ,  $Q_{O_3} = 8 \text{ mg min}^{-1}$ , and  $\text{pH} = 7.2$ .

This phenomenon was because higher  $\text{Fe}_3\text{O}_4@\text{SiO}_2@\text{CeO}_2$  dosage provided more active sites that leading to an increase in the possibility of collision among ozone, AP and  $\text{Fe}_3\text{O}_4@\text{SiO}_2@\text{CeO}_2$  catalyst, and accelerated  $\text{O}_3$  conversion into ROS for destructing organic pollutants. Thus, the AP removal rate was improved. The advantage of  $\text{Fe}_3\text{O}_4@\text{SiO}_2@\text{CeO}_2$  catalyst was also well reflected in the removal of COD. As shown in Fig. 4b, the final removal rate of COD over the mentioned range reached 13%, 15.51%, 18.03%, and 22.69%, respectively.

#### 3.2.4. Influence of cerium oxide loading

Cerium oxide loading onto magnetic  $\text{Fe}_3\text{O}_4@\text{SiO}_2$  changed the surface properties of the support material. Compared to ozonation alone, the cerium oxide loading exerted a positive influence on the AP removal (Fig. 5a), which was possibly due to the loaded rare metal. From the elementary composition, it was noticed that the proportion of Ce from  $\text{Fe}_3\text{O}_4@\text{SiO}_2@\text{CeO}_2$  catalyst increased as the cerium

oxide loading increased from 1 to 3 mmol by EDX analysis, with the minimum and maximum proportion of 1.69% and 14.72%. Certainly, the influence of the cerium oxide loading on COD removal was investigated which could be seen in Fig. 5b. It was found that the COD removal rate gradually increased. Because higher Ce loading could provide more active sites to accelerate  $\text{O}_3$  conversion into active radicals. Therefore, Ce played an important role in the catalytic ozonation process.

### 3.3. Mechanism

#### 3.3.1. Mechanism of AP degradation

GC-MS, HPLC, and IC were used to analyze the intermediates generated in the catalytic ozonation AP system. The result showed that during the AP degradation, various intermediates were detected, as shown in Table 1. These intermediates included anisole, nitrobenzene,

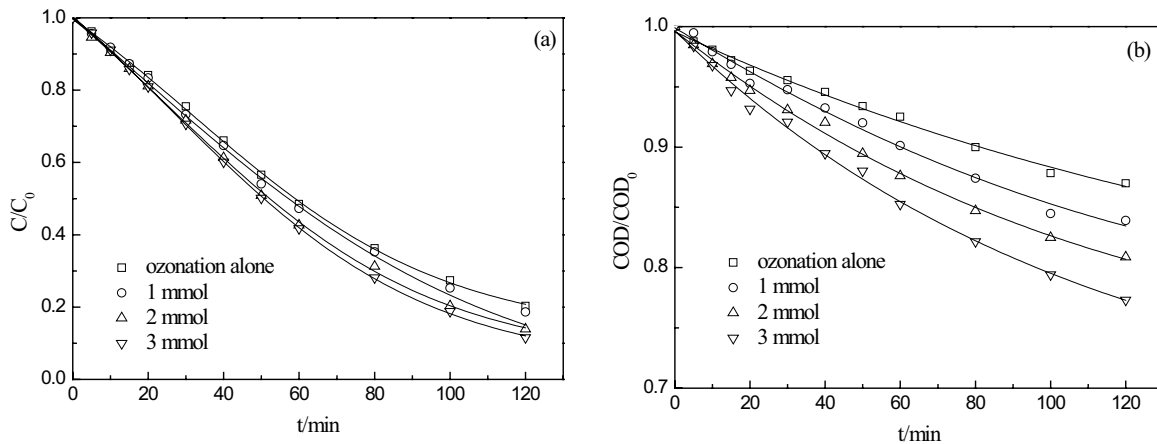


Fig. 5. Influence of the cerium oxide loading content in catalytic ozonation process: (a) AP removal and (b) COD removal. Experimental conditions:  $C_0 = 1,000 \text{ mg L}^{-1}$ ,  $Q_{O_3} = 8 \text{ mg min}^{-1}$ ,  $\text{pH} = 7.2$ , catalytic dosage  $\approx 666 \text{ mg L}^{-1}$ .

Table 1  
Intermediate products in catalytic ozonation process

Symbol	Products	Structural formula	Retention time (min)
P1	Nitrobenzene		8.28
P2	Phenol		9.02
P3	<i>N</i> -phenylpropinamide		10.61
P4	/		11.62
P5	Aniline		14.12

*n*-phenylpropinamide, aniline, and some small molecular acids. Similar results were also achieved in the reference [10,25].

During the AP degradation, ozone or free radicals would attack the C–N bond (in position one) in the branched chain

of pyrazole, phenol appeared. Nitrobenzene formed because of the attack on the N–N bond and C–N bond of pyrazole (in position two and three) and the direct oxidation of ozone or free radicals. The attack on position four led to the

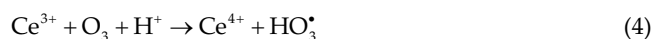
opening of pentacyclic ring, thus two new substances produced. With the reaction progressing, kinds of other intermediates were formed and the proposed degradation pathway is shown in Fig. 6.

### 3.3.2. Mechanism of $\text{Fe}_3\text{O}_4@\text{SiO}_2@\text{CeO}_2$ catalyst

Catalytic ozonation with metal oxides is a potential process to improve the degradation of recalcitrant organics [26,27]. In general, there exist two reaction mechanisms including the generation of hydroxyl radicals from ozone decomposition and direct ozone oxidation of surface metal-organic complexes [28]. In order to verify whether the catalytic ozonation of AP belongs to hydroxyl radical reaction mechanism, the experiment was carried out in the presence of *tert*-butyl alcohol (TBA). In most cases, as a hydroxyl radical scavenger, the addition of TBA inhibits the ozone decomposition and reduces the removal of organic matters [29]. To clearly investigate the contribution of  $\cdot\text{OH}$  to the mineralization of AP during the  $\text{O}_3/\text{Fe}_3\text{O}_4@\text{SiO}_2@\text{CeO}_2$  system, radical quenching experiments were carried out. TBA was selected as a  $\cdot\text{OH}$  scavenger because the consumption of TBA by  $\cdot\text{OH}$  is much faster than  $\text{O}_3$ . The presence of  $0.1 \text{ mol L}^{-1}$  TBA remarkably hindered AP degradation efficiency during the  $\text{O}_3/\text{Fe}_3\text{O}_4@\text{SiO}_2@\text{CeO}_2$  process. After 60 min of reaction, the AP removal efficiency was 82% in the absence of TBA, but severely reduced to 52% in the presence of TBA (in Fig. 7). This result revealed that  $\cdot\text{OH}$  was the main ROS during the  $\text{O}_3/\text{Fe}_3\text{O}_4@\text{SiO}_2@\text{CeO}_2$  system.

According to Fig. 1, the three magnetic catalysts showed different activities, which decreased gradually in the following order:  $\text{Fe}_3\text{O}_4@\text{SiO}_2@\text{CeO}_2 > \text{Fe}_3\text{O}_4@\text{SiO}_2 > \text{Fe}_3\text{O}_4$ . The coexistence of  $\text{Fe}^{2+}$  and  $\text{Fe}^{3+}$  in  $\text{Fe}_3\text{O}_4$  increases the decomposition of ozone [30]. While  $\text{Fe}_3\text{O}_4$  and  $\text{Fe}_3\text{O}_4@\text{SiO}_2$  catalysts only had a slight effect on AP degradation, the high efficiency should be considered to be related to the loading of Ce or the synergistic effect of metal irons. This was ascribed to the fact that the activation of  $\text{O}_3$  conversion into  $\cdot\text{OH}$  on cerium-based catalysts was along with the oxidation of  $\text{Ce}^{3+}$  by  $\text{O}_3$ . The abundant  $\pi$ - $\pi$  electrons on  $\text{Fe}_3\text{O}_4@\text{SiO}_2$  surfaces could promote the electron transfer during catalytic reaction, which thereafter resulted in the facilitated reduction of  $\text{Ce}^{3+}$  from  $\text{Ce}^{4+}$ . Through release and storage of oxygen,  $\text{CeO}_2$

can change oxidation state of lattice Ce between  $\text{Ce}^{3+}$  and  $\text{Ce}^{4+}$  and also stabilized surface metal ions with the increase content of the lattice  $\text{Ce}^{3+}$  [31]. It was considered that the mechanism of catalytic ozonation mainly consisted of the redox reaction between Ce and antipyrine, which agreed with the opinion of Delanoë et al. [32].



### 3.4. Electrical energy consumption

The economics is an important fraction for selecting any water/wastewater treatment process. The electrical energy per order (EE/O), defined as the number of kW h of electrical energy required to reduce the concentration of a pollutant by 1 order of magnitude (90%) in  $1 \text{ m}^3$  of contaminated water, was employed to assess the economics in different systems [33,34].

$$\text{EE/O} = \frac{P \times t \times 1,000}{V \times 60 \times \log\left(\frac{[C]_0}{[C]}\right)} \quad (8)$$

where  $P$  is the power input (kW) of the ozonation system for the ozone generator (0.15 kW),  $t$  is the reaction time (min),  $V$  is the volume of the simulated water in the reactor,  $[C]_0$  and  $[C]$  are the initial and final concentrations of AP.

The EE/O was estimated from kinetic rate constants. According to the above data, the kinetic rate constants were  $1.05 \times 10^{-2}$  and  $1.19 \times 10^{-2} \text{ min}^{-1}$  in ozonation and catalytic ozonation processes. Compared the energy consumption, the final result indicated that the addition of  $\text{Fe}_3\text{O}_4@\text{SiO}_2@\text{CeO}_2$  catalyst reduced 11.7%. In conclusion,

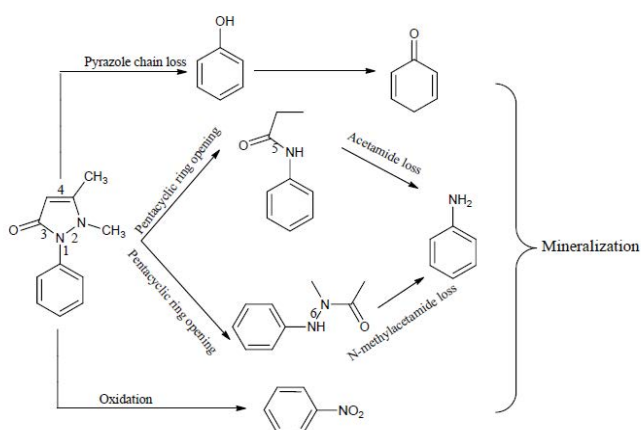


Fig. 6. Degradation of AP.

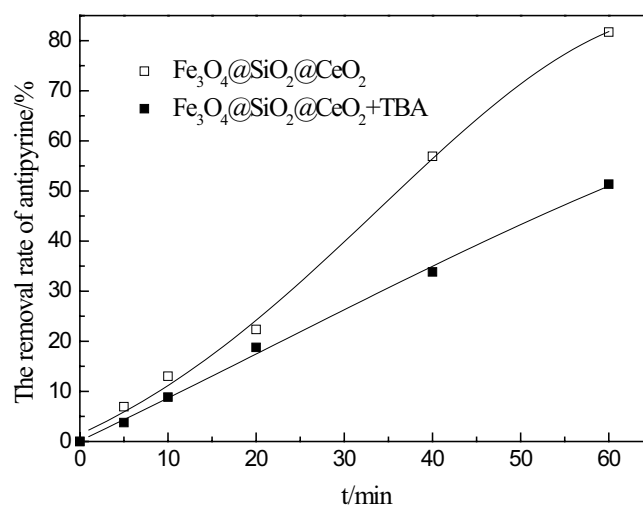


Fig. 7. Effect of TBA on the catalytic ozonation of AP.

the catalytic ozonation system was more energy saving than the ozonation system. Thus, catalytic ozonation using  $\text{Fe}_3\text{O}_4@\text{SiO}_2@\text{CeO}_2$  catalyst was considered as an economic and practical technology.

#### 4. Conclusions

This study explored the effect of catalytic ozonation AP with magnetic  $\text{Fe}_3\text{O}_4@\text{SiO}_2@\text{CeO}_2$  catalyst. The operating parameters such as initial pH, ozone dosage, initial concentration of AP, the catalyst dosage and the cerium oxide loading could greatly influence the effects of AP degradation and the optimized condition was achieved. The reaction kinetics was analyzed and the results were found to follow the pseudo-first-order kinetic model. The degradation mechanism was discussed and with the help of kinds of intermediates detected. The mechanism of catalytic ozonation mainly attributed to surface reaction of  $\text{Fe}_3\text{O}_4@\text{SiO}_2@\text{CeO}_2$  catalyst. EE/O was employed to assess the energy consumption, indicating the catalytic ozonation was more energy saving than ozonation alone.  $\text{Fe}_3\text{O}_4@\text{SiO}_2@\text{CeO}_2$  catalyst could have a prospective application in catalytic ozonation for the degradation of PPCPs, especially the refractory pharmaceutical wastewater.

#### Acknowledgments

This research was supported by Zhejiang Provincial Natural Science Foundation of China (LGJ18E080001). The authors thank professor Gu Xu at McMaster University for the assistance of the materials analysis and mechanism study.

#### References

- Rodil, J.B., Quintana, R., Cela, Transformation of phenazone-type drugs during chlorination, *Water Res.*, 46 (2012) 2457–2468.
- X. Yang, R.C. Flowers, H.S. Weinberg, P.C. Singer, Occurrence and removal of pharmaceuticals and personal care products (PPCPs) in an advanced wastewater reclamation plant, *Water Res.*, 45 (2011) 5218–5228.
- K. Kuroda, M. Murakami, K. Oguma, Y. Muramatsu, H. Takada, S. Taldzawa, Assessment of groundwater pollution in Tokyo using PPCPs as sewage markers, *Environ. Sci. Technol.*, 46 (2012) 1455–1464.
- T. Deblonde, C. Cossu-Leguille, P. Hartemann, Emerging pollutants in wastewater: a review of the literature, *Int. J. Hyg. Environ. Health*, 214 (2011) 442–448.
- C.Q. Tan, N.Y. Gao, Y. Deng, W.L. Rong, S.D. Zhou, N.X. Lu, Degradation of antipyrine by heat activated persulfate, *Sep. Purif. Technol.*, 109 (2013) 122–128.
- J.L. Liu, M.H. Wong, Pharmaceuticals and personal care products (PPCPs): a review on environmental contamination in China, *Environ. Int.*, 59 (2013) 208–224.
- K. Reddersen, T. Heberer, U. Dünnebier, Identification and significance of phenazone drugs and their metabolites in ground- and drinking water, *Chemosphere*, 49 (2002) 539–544.
- W. Li, V. Nanaboina, Q.X. Zhou, G.V. Korshin, Effects of Fenton treatment on the properties of effluent organic matter and their relationships with the degradation of pharmaceuticals and personal care products, *Water Res.*, 46 (2012) 403–412.
- Y. Xia, J.Q. Feng, S.Q. Fan, W. Zhou, Q.Z. Dai, Fabrication of a multi-layer CNT-PbO<sub>2</sub> anode for the degradation of isoniazid: kinetics and mechanism, *Chemosphere*, 263 (2021) 128069.
- H.F. Miao, M. Cao, D.Y. Xu, H.Y. Ren, M.X. Zhao, Z.X. Huang, W.Q. Ruan, Degradation of phenazone in aqueous solution with ozone: influencing factors and degradation pathways, *Chemosphere*, 119 (2015) 326–333.
- A. Duran, J.M. Monteagudo, I. Sanmartin, A. Garcia-Diaz, Sonophotocatalytic mineralization of antipyrine in aqueous solution, *Appl. Catal., B*, 138 (2013) 318–325.
- A.G. Goncalves, J.J.M. Orfao, M.F.R. Pereira, Catalytic ozonation of sulphamethoxazole in the presence of carbon materials: catalytic performance and reaction pathways, *J. Hazard. Mater.*, 239 (2012) 167–174.
- A. Shokri, Degradation of 2-nitrophenol from petrochemical wastewater by ozone, *Russ. J. Appl. Chem.*, 88 (2015) 2038–2043.
- A. Shokri, A.H. Joshagani, Using microwave along with TiO<sub>2</sub> for degradation of 4-chloro-2-nitrophenol in aqueous environment, *Russ. J. Appl. Chem.*, 89 (2016) 1985–1990.
- A. Shokri, The treatment of spent caustic in the wastewater of olefin units by ozonation followed by electrocoagulation process, *Desal. Water Treat.*, 111 (2018) 173–182.
- J. Akhtar, N.S. Amin, A. Aris, Combined adsorption and catalytic ozonation for removal of sulfamethoxazole using Fe<sub>3</sub>O<sub>4</sub>/CeO<sub>2</sub> loaded activated carbon, *Chem. Eng. J.*, 170 (2011) 136–144.
- J. Vittenet, W. Aboussaoud, J. Mendret, J.S. Pic, H. Debellefontaine, N. Lesage, K. Faucher, M.H. Manero, F. Thibault-Starzyk, H. Leclerc, A. Galarneau, S. Brosillon, Catalytic ozonation with gamma-Al<sub>2</sub>O<sub>3</sub> to enhance the degradation of refractory organics in water, *Appl. Catal., A*, 504 (2015) 519–532.
- P. Pocostales, P. Alvarez, F.J. Beltran, Catalytic ozonation promoted by alumina-based catalysts for the removal of some pharmaceutical compounds from water, *Chem. Eng. J.*, 168 (2011) 1289–1295.
- S. Capone, M.G. Manera, A. Taurino, P. Siciliano, R. Rella, S. Luby, M. Benkovicova, P. Siffalovic, E. Majkova, Fe<sub>3</sub>O<sub>4</sub>/gamma-Fe<sub>2</sub>O<sub>3</sub> nanoparticle multilayers deposited by the Langmuir-Blodgett technique for gas sensors application, *Langmuir*, 30 (2014) 1190–1197.
- Y.H. Deng, C.C. Wang, J.H. Hu, W.L. Yang, S.K. Fu, Investigation of formation of silica-coated magnetite nanoparticles via sol-gel approach, *Colloid Surf., A*, 262 (2005) 87–93.
- W.W. Li, Z.M. Qiang, T. Zhang, F.L. Cao, Kinetics and mechanism of pyruvic acid degradation by ozone in the presence of PdO/CeO<sub>2</sub>, *Appl. Catal., B*, 113 (2012) 290–295.
- Q.Z. Dai, J.Y. Wang, J. Yu, J. Chen, J.M. Chen, Catalytic ozonation for the degradation of acetylsalicylic acid in aqueous solution by magnetic CeO<sub>2</sub> nanometer catalyst particles, *Appl. Catal., B*, 144 (2014) 686–693.
- H. Ding, Y. Zhao, Q. Duan, J. Wang, K. Zhang, G. Ding, X. Xie, C. Ding, Efficient removal of phosphate from aqueous solution using novel magnetic nanocomposites with Fe<sub>3</sub>O<sub>4</sub>@SiO<sub>2</sub> core and mesoporous CeO<sub>2</sub> shell, *J. Rare Earth*, 35 (2017) 984–994.
- G. Cheng, J.L. Zhang, Y.L. Liu, D.H. Sun, J.Z. Ni, Synthesis of novel Fe<sub>3</sub>O<sub>4</sub>@SiO<sub>2</sub>@CeO<sub>2</sub> microspheres with mesoporous shell for phosphopeptide capturing and labeling, *Chem. Commun.*, 47 (2011) 5732–5734.
- M.S. Du, K.P. Chen, Y.P. Lin, Degradation of ibuprofen and acetylsulfamethoxazole by multi-walled carbon nanotube catalytic ozonation: surface properties, kinetics and modeling, *Environ. Sci. Water Res. Technol.*, 5 (2019) 1758–1768.
- C. von Sonntag, U. von Gunten, *Chemistry of Ozone in Water and Wastewater Treatment: From Basic Principles to Applications*, IWA Publishing, London, 2012.
- L. Yang, C. Hu, Y.L. Nie, J.H. Qu, Catalytic ozonation of selected pharmaceuticals over mesoporous alumina-supported manganese oxide, *Environ. Sci. Technol.*, 43 (2009) 2525–2529.
- T. Zhang, W.W. Li, J.P. Croue, Catalytic ozonation of oxalate with a cerium supported palladium oxide: an efficient degradation not relying on hydroxyl radical oxidation, *Environ. Sci. Technol.*, 45 (2011) 9339–9346.
- J. Nawrocki, B. Kasprzyk-Hordern, The efficiency and mechanisms of catalytic ozonation, *Appl. Catal., B*, 99 (2010) 27–42.

- [29] Q.Z. Dai, L.L. Chen, S.J. Zhou, J.M. Chen, Kinetics and mechanism study of direct ozonation organics in aqueous solution, *RSC Adv.*, 5 (2015) 24649–24654.
- [30] A.H. Lv, C. Hu, Y.L. Nie, J.H. Qu, Catalytic ozonation of toxic pollutants over magnetic cobalt-doped  $\text{Fe}_3\text{O}_4$  suspensions, *Appl. Catal., B*, 117 (2012) 246–252.
- [31] A.D. Mayernick, M.J. Janik, Methane oxidation on Pd-Ceria: a DFT study of the mechanism over  $\text{Pd}_x\text{Ce}_{1-x}\text{O}_2$ , Pd, and PdO, *J. Catal.*, 278 (2011) 16–25.
- [32] F. Delanoe, B. Acedo, N.K.V. Leitner, B. Legube, Relationship between the structure of Ru/CeO<sub>2</sub> catalysts and their activity in the catalytic ozonation of succinic acid aqueous solutions, *Appl. Catal. B*, 29 (2001) 315–325.
- [33] Y.J. Xia, X.Z. Bian, Y. Xia, W. Zhou, L. Wang, S.Q. Fan, P. Xiong, T.T. Zhan, Q.Z. Dai, J.M. Chen, Effect of indium doping on the  $\text{PbO}_2$  electrode for the enhanced electrochemical oxidation of aspirin: an electrode comparative study, *Sep. Purif. Technol.*, 237 (2020) 116321, doi: 10.1016/j.seppur.2019.116321.
- [34] J.C. Crittenden, R.R. Trussell, K.J. Howe, *Water Treatment-Principles and Design*, 3rd ed., John Wiley & Sons Inc., Hoboken, NJ, 2012.